Comparison of image and data domain methods for three-material decomposition in dual-energy CT

T. Humphries, R. McGarity and K. Uy

***Abstract*—In this work we propose a novel three-material decomposition method in the data domain which is based on a conservation of volume constraint. We compare the approach with an image-based decomposition method using a recently proposed polyenergetic reconstruction algorithm to generate the reconstructed images. Our preliminary results indicate that the image-based decomposition using polyenergetic reconstruction provides better image quality than the data-domain approach.**

I. Introduction

Since the early days of CT imaging it has been known that a decomposition of an image into two components (e.g. soft tissue and bone) can be recovered from dual-energy CT (DECT) measurements. Recovering a decomposition of a third material, such as fat or contrast agent, from DECT data is only possible with the inclusion of additional constraints. One approach which can be physically justified is to utilize conservation of volume to require that the volume fraction of each material sum to one in every pixel of the image [1]. A simple image-domain approach to three-material decomposition consists of reconstructing images based on the high and low-energy data sets, and then solving a three-by-three linear system of equations.

One drawback of an image-based approach is that the images reconstructed from the high and low energy data sets may contain artifacts, such as those caused by beam hardening. Since the material decomposition problem is typically ill-conditioned, even small errors in these images may produce large errors in the material decomposition. An alternative is to use a data-domain approach to material decomposition instead. In such an approach, one solves a nonlinear system of equations for each set of measurements to estimate the equivalent length of each material through which the beam passed. This process yields a set of "material sinograms" which can then be used to reconstruct material images using a conventional reconstruction algorithm. Drawbacks of this approach include the increased computation required to solve a nonlinear system of equations, and the requirement that the two sets of measurements be acquired along the same lines. By directly modeling X-ray polychromaticity, however, the approach is able to avoid the issue of beam hardening.

The data domain approach has been proposed previously for two-material decompositions [2]. Three-material decompositions in the data domain have also been proposed [3] but are not widely used. In this work we propose a novel three-material decomposition method in the data domain which is based on the conservation of volume constraint. We compare the approach with an image-based decomposition method using a recently proposed polyenergetic iterative reconstruction algorithm to generate the reconstructed images. Our results indicate that by compensating adequately for beam hardening effects, the image-based decomposition using polyenergetic reconstruction provides better image quality than the data-domain approach.

School of STEM, University of Washington Bothell, Bothell, WA, USA

II. Methodology

A. Image domain decomposition

Let $h = 1, 2$ denote the low and high-energy measurements, and let $i = 1, 2, 3$ denote the three materials assumed to be present in the object. Then, the set of dual-energy measurements along line j can be represented as:

$$I_{h,j} = \int S_h(E) \cdot \exp\left[\sum_{i=1}^{3} -\mu_i(E)\delta_{i,j}\right] dE, \qquad (1)$$

where $S_h(E)$ refers to the energy spectrum of the beam at energy h, $\mu_i(E)$ is the energy-dependent linear attenuation coefficient of the ith material at its nominal density, and $\delta_{i,j}$ represents the equivalent length of intersection of material i with line j. The use of linear attenuation coefficient rather than mass attenuation coefficient is motivated by the use of conservation of volume as a third constraint [1]. An image-based decomposition approach uses these data sets to reconstruct two images of the object, one corresponding to the high energy, and one to the low energy. Each image is presumed to represent the attenuation map of the object at some reference energy. We use E_h to denote this reference energy, and ν_h to denote the reconstructed attenuation map at that energy. Using conservation of volume, the volume fraction $f_{i,k}$ of each material in pixel k is then computed by solving a linear system:

$$\begin{bmatrix} \mu_1(E_1) & \mu_2(E_1) & \mu_3(E_1) \\ \mu_1(E_1) & \mu_2(E_2) & \mu_3(E_2) \\ 1 & 1 & 1 \end{bmatrix} \begin{bmatrix} f_{1,k} \\ f_{2,k} \\ f_{3,k} \end{bmatrix} = \begin{bmatrix} \nu_{1,k} \\ \nu_{2,k} \\ 1 \end{bmatrix}, \qquad (2)$$

The images f_i then provide material decomposition images of the ith material. This system tends to be ill-conditioned, in particular if the energies E_1 and E_2 are close to one another, or if any of the three materials have similar attenuation coefficients. As a result, artifacts in the images ν_h introduced from sources such as beam hardening may cause significant errors in the reconstructed material decompositions f_i. Techniques such as soft-tissue correction which are applied before reconstruction using a conventional algorithm (e.g. filtered

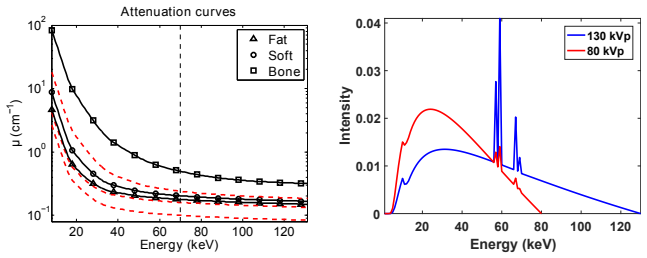

Fig. 1. Left: Illustration of how pSART using linear interpolation between basis material curves (black lines) to determine energy-dependent attenuation function in other pixels (red dashed lines). Interpolation weights are determined from values at the reference energy (70 keV in this example). Right: High and low energy spectra used in phantom experiments.

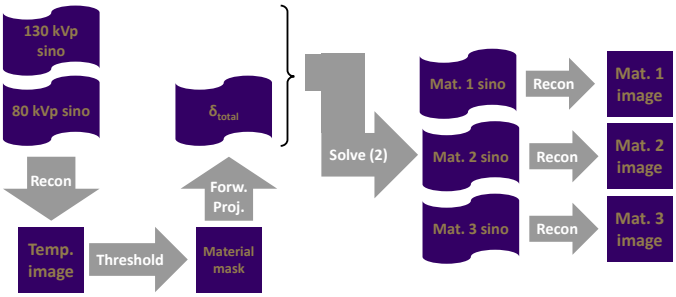

Fig. 2. Flowchart of proposed data domain decomposition.

back projection (FBP)) only provide approximate correction for beam hardening.

In this paper we apply the polyenergetic SART (pSART) algorithm [4] to reconstruct the images ν_h. pSART is a variation on the simultaneous algebraic reconstruction technique (SART) which incorporates a polyenergetic forward projection model. This polyenergetic forward projection is based on linear interpolation between attenuation curves for known basis materials such as soft tissue, bone, and contrast agent. In essence, the reconstructed attenuation coefficient of every pixel at the reference energy E_h determines a linear interpolation weighting which is used to determine the attenuation coefficient of that pixel at every other energy. The interpolation is performed based on the assumption that pixels may contain mixtures of up to two basis materials with adjacent linear attenuation coefficients, as well as the assumption that bone and contrast agent do not mix. See (Fig. 1) for an illustration. Our reconstruction algorithm also incorporates total variation (TV) minimization, as described in [5]. At every iteration of the algorithm, the TV of the image is reduced in an effort to suppress noise, which also diminishes the accuracy of the decomposition.

B. Data domain decomposition

Our data domain decomposition method is based on the observation that integrating the third equation in (2) leads to the constraint

$$\delta_{1,j} + \delta_{2,j} + \delta_{3,j} = \delta_{\text{total},j}, \tag{3}$$

where $\delta_{\text{total},j}$ is the total amount of material through which line j passes. Together with the two nonlinear equations specified in (1), this gives a 3×3 system of nonlinear equations which can be solved for the δ_i. These δ_i can then be used as input to a conventional reconstruction algorithm (e.g. FBP or SART) to recover maps of the material fractions f_i of every material. By directly modeling X-ray polychromaticity in equations (1), this method avoids the issue of beam hardening artifacts. One difficulty, however, is that the value of $\delta_{\text{total},j}$ is not known *a priori* and must be estimated for each measurement j. Our approach is to reconstruct a preliminary image of the object based on either the low or high-energy measurements, after soft tissue correction. The image is then thresholded to obtain a material mask which indicates which pixels in the image contain material and which do not. The mask contains values between 0 and 1, with fractional values assigned to edges to account for partially filled pixels. This mask is then forward-projected to generate an estimate for $\delta_{\text{total},j}$ for each measurement. This process is illustrated in (Fig. 2) below.

It should be noted that since (3) is obtained from integrating the sum-to-one constraint in (2), it does not actually require the reconstructed material fractions to sum to one in every pixel of the image; however, one expects this to roughly be the case if the data are consistent. Additionally, the Jacobian matrix of the nonlinear system (1), (3), if simplified using the mean value theorem for integrals, yields a matrix that is essentially the same as that on the left side of (2). Thus the conditioning of the data-domain decomposition problem is also poor, and the problem is sensitive to noise in the projection data and error in estimating $\delta_{\text{total},j}$.

III. Numerical Experiments

We first perform numerical experiments on a 200×200 pixel phantom (pixel size 1.5mm). The phantom models a ellipsoid consisting primarily of soft tissue, with several smaller ellipsoidal regions containing mixtures of materials. The small ellipsoid on the right side of the phantom contains air, which complicates the process of computing $\delta_{\text{total},j}$ for lines passing through that region. To test the performance of the algorithm, we considered two different sets of materials; (1) soft tissue, bone, and fat, and (2) soft tissue, bone, and iodine contrast. The first problem is more ill-conditioned as the attenuation curves of soft tissue and fat are very similar. Projection data were simulated based on a low energy spectrum of 80 kVp and a high-energy spectrum of 130 kVp, with noise proportional to an initial intensity of $\int S(E)\, dE = 1 \times 10^6$ for both spectra. Mass attenuation curves and densities for the different materials, and the two energy spectra (shown in (Fig. 1)), were obtained from the Michigan Image Reconstruction Toolbox [6].

For the image-domain decomposition, the images ν_i were reconstructed using pSART with TV minimization with reference energies $E_1 = 50$ keV and $E_2 = 80$ keV. For the data-domain decomposition, the preliminary image used to estimate $\delta_{\text{total},j}$ was reconstructed using SART. Following the determination of the $\delta_{i,j}$ by solving the nonlinear system of equations, the material decomposition images were reconstructed using SART with TV minimization, to suppress noise. The results of the experiments are shown in (Fig. 3).

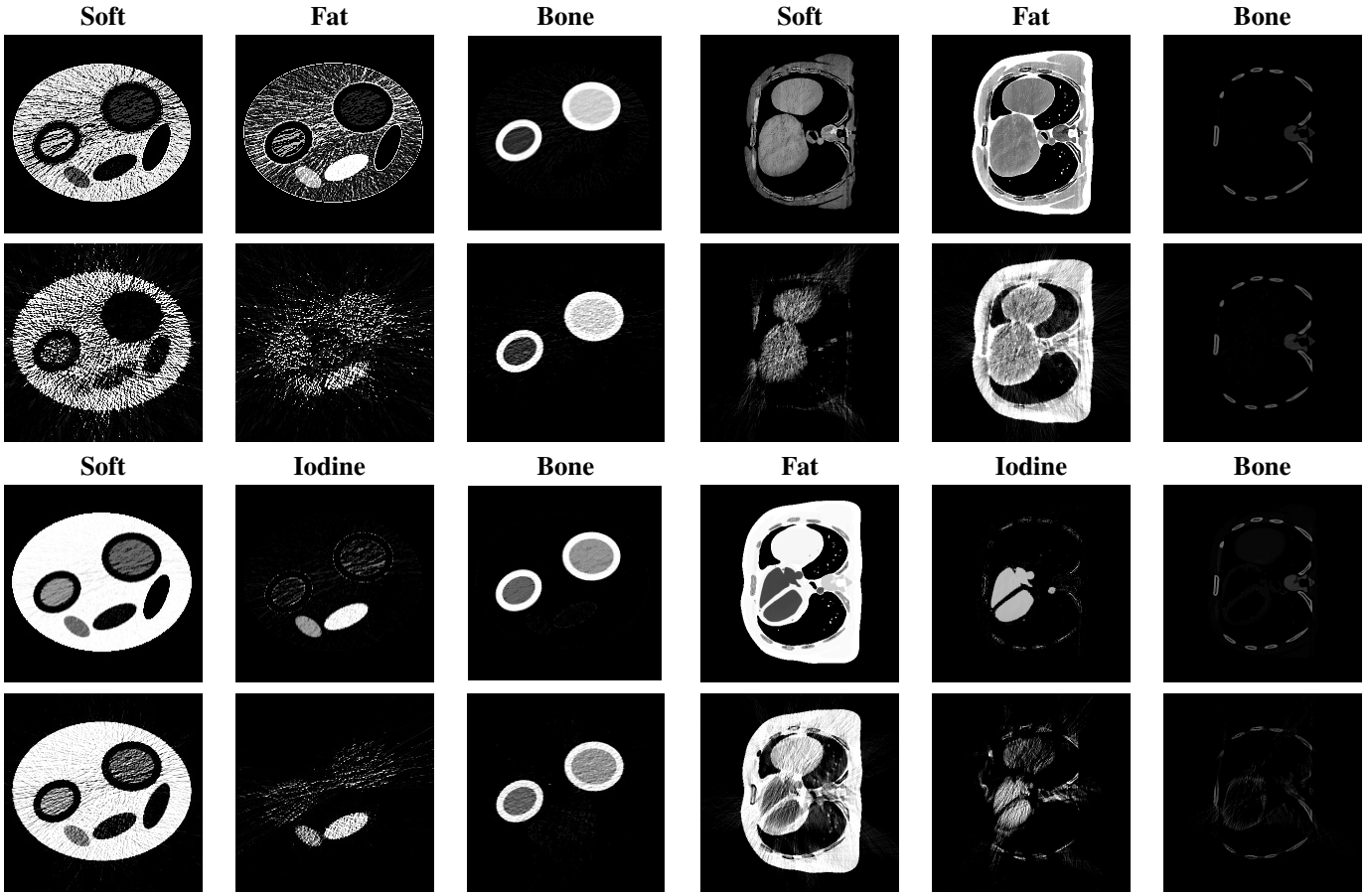

Fig. 3. Reconstructed material decompositions of simple phantom. First row: image-domain decomposition using soft tissue, fat, and bone as materials, respectively. Second row: same phantom with data-domain decomposition. Third row: image-domain decomposition using soft tissue, iodine, and bone as materials, respectively. Fourth row: same phantom with data-domain decomposition. All figures shown on a greyscale window of $[0, 1]$.

Fig. 4. Reconstructed material decompositions of XCAT phantom. First row: image-domain decomposition using soft tissue, fat, and bone as materials, respectively. Second row: same phantom with data-domain decomposition. Third row: image-domain decomposition using fat, iodine, and bone as materials, respectively. Fourth row: same phantom with data-domain decomposition. All figures shown on a greyscale window of $[0, 1]$.

From the presented results it is clear that decomposing the image into fat, soft tissue and bone is a more challenging task than decomposing it into iodine, soft tissue and bone; this is not surprising as the similarity between fat and soft tissue results in a more ill-conditioned problem. It appears as well that the image based decomposition provides better results overall; the images are less noisy, particularly for the decomposition into fat, soft tissue and bone. In this experiment, pSART is successful in reducing beam hardening artifacts to the extent that their effect is not apparent in the material decompositions. A major difficulty of the data domain approach is the difficulty in estimating $\delta_{\text{total},j}$ from the masked image; we found it difficult to obtain sufficiently accurate estimates from the preliminary reconstructed image, in light of the ill-conditioning of the problem.

As a second experiment, we tested the method on a 2D slice from the XCAT phantom [7] at a resolution of 400×400 pixels (pixel size of 0.96mm). The XCAT phantom represented a more challenging test case as it consists of many more than three tissue types and features a more realistic geometry than the simple phantom. The phantom also includes the option to include iodine contrast in the blood. As in the simple phantom experiments, we tested two different sets of basis materials: (1) soft tissue, bone, and fat, and (2) fat, bone, and iodine contrast. Fat was chosen as a reference material in the second set because it has the lowest attenuation coefficient of any of the soft tissue-like tissues in the phantom. For the purposes of our experiments, the lungs were filled with air and thus not treated as containing tissue.

The results of the experiment are shown in (Fig. 4). In this instance the image-domain decomposition has clearly produced better results, particularly for the soft tissue decomposition in the first experiment, and the iodine decomposition in the second experiment. In this case the determination of $\delta_{\text{total},j}$ was particularly error prone due to the complicated geometry of the lungs. We note that the image domain decomposition appears to be largely free of artifacts caused by beam hardening, as a result of the use of the pSART algorithm.

IV. Conclusions

In this paper we have presented a novel method for performing three-material decomposition in the data domain using DECT. The method is based on integrating a conservation of volume constraint along lines and solving the resulting 3×3 nonlinear system of equations to obtain material sinograms,

which can be reconstructed using conventional means. Forming the system of nonlinear equations requires estimating the total length of material passed through by each ray, which we do by forward-projecting a mask based on a thresholded image.

In numerical experiments we compare the performance of the method with a conventional image-domain decomposition which includes polyenergetic modeling and TV minimization when reconstructing the initial images. In our experiments the image-domain approach provides higher-quality, less noisy decompositions than the data-domain approach. A key difficulty in the data-domain approach is the need to estimate the total length of material, which is prone to error and results in significant degradation of the decompositions due to the ill conditioning of the problem.

REFERENCES

[1] P.R.S. Mendonca, P. Lamb, and D.V. Sahani. A flexible method for multi-material decomposition of dual-energy CT images. *IEEE Trans. Med. Imag.*, 33(1):99–116, Jan 2014.

[2] L.A. Lehmann, R.E. Alvarez, A. Macovski, W.R. Brody, N.J. Pelc, S.J. Riederer, and A.L. Hall. Generalized image combinations in dual kvp digital radiography. *Medical Physics*, 8(5):659–667, 1981.

[3] L. Yu, X. Liu, and C. McCollough. Pre-reconstruction three-material decomposition in dual-energy CT. In *Proceedings of SPIE*, volume 7258, pages 72583V–72583V, 2009.

[4] Y. Lin and E. Samei. An efficient polyenergetic SART (pSART) reconstruction algorithm for quantitative myocardial CT perfusion. *Med. Phys.*, 41(2):021911–1 – 021911–14, 2014.

[5] T. Humphries and A. Faridani. Reconstruction of sparse-view polyenergetic CT data using total variation minimization. In *2015 IEEE Nuclear Science Symposium Conference Record*, 2015.

[6] J. Fessler. Michigan image reconstruction toolbox. http://web.eecs.umich.edu/∼fessler/code/.

[7] W.P. Segars, G. Sturgeon, S. Mendonca, J. Grimes, and B.M.W. Tsui. 4D XCAT phantom for multimodality imaging research. *Medical Physics*, 37(9):4902–4915, 2010.